# SCS+C: A Modified Sun-Canopy-Sensor Topographic Correction in Forested Terrain

Scott A. Soenen, Derek R. Peddle, *Member, IEEE*, and Craig A. Coburn, *Member, IEEE*

***Abstract*—Topographic correction based on sun-canopy-sensor (SCS) geometry is more appropriate than terrain-based corrections in forested areas since SCS preserves the geotropic nature of trees (vertical growth) regardless of terrain, view, and illumination angles. However, in some terrain orientations, SCS experiences an overcorrection problem similar to other simple photometric functions. To address this problem, we propose a new SCS+C correction that accounts for diffuse atmospheric irradiance based on the C-correction. A rigorous, comprehensive, and flexible method for independent validation based on canopy geometric optical reflectance models is also introduced as an improvement over previous validation approaches, and forms a secondary contribution of this paper. Results for a full range of slopes, aspects, and crown closures showed SCS+C provided improved corrections compared to the SCS and four other photometric approaches (cosine, C, Minnaert, statistical-empirical) for a Rocky Mountain forest setting in western Canada. It was concluded that SCS+C should be considered for topographic correction of remote sensing imagery in forested terrain.**

***Index Terms*—Canopy reflectance model, forests, radiometric processing, Rocky Mountains, sun-canopy-sensor (SCS), SCS with C-correction (SCS+C), topographic correction.**

## I. Introduction

REMOTE sensing image analysis can be adversely affected by the influence of terrain slope and aspect on recorded sensor signal response [1]–[3]. Differences in terrain orientation often create variation in signal values between pixels with similar land cover and biophysical-structural properties as a result of differences in irradiance owing to the angle of incident illumination ($i$), and differences in radiance according to the angle of exitance ($e$). For non-Lambertian surfaces, the reflected radiance is also affected by the intrinsic reflective properties of the surface described by the bidirectional reflectance distribution function (BRDF) [4]. In forested areas, this topographic effect also modifies the subpixel scale shadowing [5] that has been shown to provide improved estimates of important biophysical and structural information using spectral mixture analysis and canopy reflectance models [6]–[8], [26]–[29], [37].

Early photometric techniques developed to reduce this topographic effect include the cosine, Minnaert, statistical-empirical, and C-corrections [1]–[3]. These techniques have been applied in forested areas [1]–[3], [9], [11] and are based on an implicit assumption that the geometry of terrain and trees is consistent. However, this is not the case due to the geotropic nature of trees where growth is vertical and oriented with the gravitational field, and is therefore not normal to a sloped surface as is assumed in photometric models [Fig. 1(a) and (b)]. The primary level of radiative interaction in forests is with trees and tree crowns, which have a vertical orientation regardless of terrain slope [Fig. 1(c)].

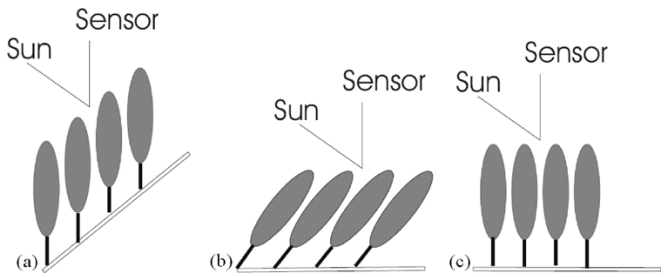


Fig. 1. Visual representation of sun-terrain-sensor geometry and sun-canopy sensor geometry. (a) Forest stand on sloped terrain. (b) STS: terrain rotated to horizontal with illumination geometry compensation based on photometric function. (c) SCS: forest stand on horizontal terrain with forest structure and orientation preserved.

As a result, a correction model that normalizes the *sun-canopy-sensor* (SCS) geometry should more effectively remove the topographic effect than traditional correction methods based on bulk *sun-terrain-sensor* (STS) geometry [5]. The SCS model by Gu and Gillespie [5] introduced this by normalizing the sunlit area within a pixel without changing the sun and sensor positions or the orientation, geometry, and structure of the canopy. It is therefore a more appropriate framework for terrain correction in forested areas. However, for some terrain orientations, the SCS model overestimates radiance, a problem common with earlier photometric models that do not characterize diffuse radiation properly (e.g., cosine correction [12], [13]).

In this study, we introduce a modification to the SCS model to better characterize diffuse irradiance by introducing a semiempirical moderator (C) to account for diffuse radiation. This follows the work of Teillet *et al.* [2] who proposed the C-correction formulation as an improvement to the earlier cosine correction. This new SCS+C correction was tested and compared with five other topographic correction approaches (cosine, Minnaert, statistical-empirical, C-correction, and SCS) for a comprehensive range of terrain and forest structural conditions generated using the Li–Strahler geometric optical mutual shadowing (GOMS) model [14] within the context of Rocky Mountain forests in

Manuscript received September 16, 2004; revised February 23, 2005. This research was supported in part by the following: Natural Sciences and Engineering Research Council of Canada (NSERC), the Water Institute for Semiarid Ecosystems (WISE), the Prairie Adaptation Research Collaborative (PARC), the Alberta Ingenuity Centre for Water Research (AICWR), Natural Resources Canada, and the Alberta Research Excellence Program.

The authors are with the Department of Geography, University of Lethbridge, Lethbridge, AB T1K 3M4, Canada (e-mail: derek.peddle@uleth.ca).

Digital Object Identifier 10.1109/TGRS.2005.852480

western Canada. We also introduce a powerful approach for topographic correction validation based on the independent use of canopy reflectance models. These models permit rigorous and comprehensive testing over a full range of terrain and forest structural settings, which has not been possible using previous validation methods.

## II. Topographic Correction

Topographic correction of remotely sensed imagery received considerable attention in the early 1980s through the development of a variety of photometric techniques [1]–[4], [10], [12], [16]. These methods were applied and tested in various studies that followed [9], [15], [17], [19]–[22]; however, no fundamentally new approaches were forthcoming until the introduction of a physical-structural basis to topographic correction by Gu and Gillespie [5] for forested terrain, follow-up studies [30] and variations to that approach [8], [29]. Current topographic correction approaches are reviewed next, to set the context for introducing SCS+C as an improved, physically based correction.

### A. Cosine Correction

The cosine correction [2], [3], [10] is a simple photometric function that, in the case of illumination not originating from the zenith, normalizes the reflectance of any pixel based on the assumption that the total irradiance received at a pixel is directly proportional to the cosine of the incidence angle ($i$) [defined as the angle between the normal to the pixel surface and the solar zenith direction [2]; see Fig. 1(a)] as

$$L_n = L\frac{\cos\theta}{\cos i} \tag{1}$$

where $L_n$ is the normalized reflectance,[1] $L$ is the uncorrected reflectance, and $\theta$ is the solar zenith angle (SZA). However, the cosine model does not take into account diffuse irradiance from atmospheric and terrain sources [15]–[17]. As a result, areas that are weakly illuminated by direct irradiance can still receive a considerable proportion of diffuse radiation and are therefore brightened excessively by the cosine correction [9]. This overcorrection is most pronounced at angles of incidence approaching 90°, where the correction factor becomes very large [2].

### B. Minnaert Correction

The Minnaert correction [2], [3], [10] was designed to address the problem that the cosine correction relies upon the Lambertian assumption (perfectly diffuse reflector), which is not applicable to most natural surfaces [2], [9]. The Minnaert [18] constant ($k$) has been used in topographic corrections to represent the extent to which a surface is non-Lambertian. While the Minnaert constant does not represent the direction of preferred scattering it does give an indication of the strength of the relationship between radiance and view angle [1]. The value of the Minnaert constant will range from 0 (specular reflector) to 1 (Lambertian surface). The Minnaert constant $k$ can be derived by first linearizing the equation

$$L = L_n(\cos^k i)(\cos^{k-1} e) \tag{2}$$

where $e$ is the exitance angle, which in the case of a nadir view angle is equivalent to the slope angle [3], [11]. The regression value for $k$ is then obtained using

$$L(\cos e) = L_n(\cos^k i)(\cos^{k-1} e) \tag{3}$$

$$\mathrm{Log}(L\cos e) = \log L_n + (k)\log(\cos i\cos e) \tag{4}$$

to solve for $k$, as the slope of the regression line [11]. The value of $k$ can then be used as a moderator [9] for the cosine equation, as

$$L_n = L\left[\frac{\cos\theta}{\cos i}\right]^k. \tag{5}$$

In the case of lower $k$ values, the denominator is increased and counteracts the overcorrection that occurs when the incidence angle approaches 90°. In several studies, the Minnaert correction has provided improved results compared to the simple cosine correction [1], [9], [11], [19]–[22].

### C. Statistical-Empirical Correction

Past studies have demonstrated that some correlation exists between the predicted illumination derived from a digital elevation model and the measured illumination of a target [2], [9]. Based on this correlation, a statistical-empirical approach was developed [2] that can be used with a linear regression to correct or normalize observed data. A regression between the cosine of the effective angle of incidence and the measured radiance will generally show a positive linear correlation. This regression line can be rotated to the horizontal to normalize the data using the equation

$$L_n = L - \cos i\, b - a + L_{\mathrm{avg}} \tag{6}$$

where $L_n$ is the normalized radiance, $a$ and $b$ are the $y$-intercept and slope of the regression line, respectively, and $L_{\mathrm{avg}}$ is the average of the measured radiance data. The rotation of the data makes an object's radiance independent of $\cos i$. As a result, the object should show the same radiance throughout the scene, regardless of terrain. While this technique is dependent on the strength of the correlation between modeled and measured illumination, it has provided image corrections similar to the Minnaert correction [9].

### D. C-Correction

Teillet *et al.* [2] proposed the addition of a semiempirical moderator (C) to the cosine correction. Based on an examination of image data, a linear relationship exists between $L$ and $\cos i$ in the form

$$L = a + b\cos i. \tag{7}$$

[1]The term "reflectance" is used in this general context for describing topographic corrections—however, these equations and concepts are applicable to raw, uncalibrated signal data, calibrated radiance and irradiance values, and to surface reflectance.

The parameter C is a function of the regression slope ($b$) and intercept ($a$)

$$\mathrm{C} = \frac{a}{b} \tag{8}$$

and is introduced to the cosine correction model as an additive term

$$L_n = L\frac{\cos\theta + \mathrm{C}}{\cos i + \mathrm{C}}. \tag{9}$$

The parameter C is said to be analogous to the effects of diffuse sky irradiance, although the analogy is not exact [2]. The C value, which may also be obtained from the slope and intercept of the regression line from the statistical-empirical approach, exerts a moderating influence on the cosine correction by increasing the denominator and reducing the overcorrection of faintly illuminated pixels. The C-correction has been shown to retain the spectral characteristics of the data and improve overall classification accuracy in areas of rugged terrain, and it can be derived easily [9], [23].

### *E. Sun-Canopy-Sensor Correction*

The SCS correction [5] improves on the cosine correction by normalizing the illuminated canopy area, which is one of the main factors contributing to pixel-level reflectance in forested scenes [5], [24], [31]. The SCS correction is equivalent to projecting the sunlit canopy from the sloped surface to the horizontal, in the direction of illumination. Assuming that the reflected radiation from the sunlit canopy is largely independent of topography due to the geotropic (vertical) nature of tree growth, the integrated reflectance from the sunlit canopy is proportional to its area

$$L_n = L\frac{\cos\alpha\cos\theta}{\cos i} \tag{10}$$

where $\alpha$ is the terrain slope [5]. Because the sun-crown geometry is preserved [Fig. 1(c)], the SCS model is more appropriate physically compared to the aforementioned corrections, and therefore should be superior for topographic correction in forested scenes. However, by formulating the SCS model to be as generally applicable as possible, the effect of diffuse irradiance is neglected resulting in overcorrection for slopes facing away from the source of illumination. This sets the context for our modified SCS formulation.

### *F. SCS+C Correction*

The cause of the overcorrection in the SCS model is similar to that with the cosine correction. As the angle of incidence approaches 90°, the correction factor becomes excessively large. In the C-correction, the parameter C has been shown to have a moderating influence on the cosine correction by emulating the effect of diffuse sky illumination [2], [9]. Here, we propose the SCS+C correction where the moderator C is derived using (7) and (8) but within the improved physical context of the SCS model. This addition is intended to be an improvement to the SCS correction in a similar way as the C-correction improves on the cosine correction. The formulation for this new SCS+C correction is

$$L_n = L\frac{\cos\alpha\cos\theta + \mathrm{C}}{\cos i + \mathrm{C}}. \tag{11}$$

The parameter C was chosen due to its past success in moderating the cosine correction [9], [23] and also because of its computational simplicity [2]. While other parameters that account for diffuse atmospheric and terrain radiance may provide additional refinements, the computational costs and input parameter requirements may be impractical and not consistent with the fundamental philosophy of general applicability of the SCS model as proposed by Gu and Gillespie [5].

## III. Experimental Design

### *A. Topographic Correction Data and Model-Based Validation*

To provide a comprehensive test and comparison of the new SCS+C correction, a simulated reflectance dataset was generated over a full range of terrain orientations and forest structures using a canopy reflectance model. A key feature of this approach is the ability to compute modeled reflectance data at different slopes, aspects, and stand densities, and to then derive the corresponding reflectance values for flat terrain based on the identical forest structure, component spectral response, and illumination geometry (i.e., slope and aspect are set to flat terrain; all other model parameters unchanged). This provided an internally consistent and fully independent approach for validation and evaluation of the different topographic correction methods where each of the various terrain normalized results are compared against the modeled reflectance values for flat terrain. Thus, the GOMS-modeled reflectance values for flat terrain served as the topographically normalized (corrected) reflectance to which all sloped reflectance values should ideally be corrected.

The Li and Strahler [14] geometric optical mutual shadowing (GOMS) model was selected as the canopy reflectance model for the validation owing to its advantages over other reflectance models, such as: 1) its explicit inclusion of slope and aspect as an input parameter in its formulation; 2) the ability to evaluate illumination-crown geometry as a function of terrain and illumination conditions [25], [32]; 3) it accounts for complex canopy mutual shadowing that is common in mountainous terrain and which is directly influenced by stand structure, terrain and illumination conditions and can significantly affect pixel-level reflectance [14]; and, 4) the GOMS model is relatively easy to parameterize and has been shown to be superior to models using other geometric shapes to represent forest crowns [7]. The topographic component of the GOMS model has been proven sound both theoretically [25], [36] and in an extensive set of different tests [8], [32]–[35]. When using GOMS for validation of topographic corrections, one should be aware that the GOMS model assumes the pixel size is greater than individual canopy elements [14]. As a result, the model cannot account for small topographic variations found in complex terrain. Also, as with all the other corrections tested in this study, the GOMS model does

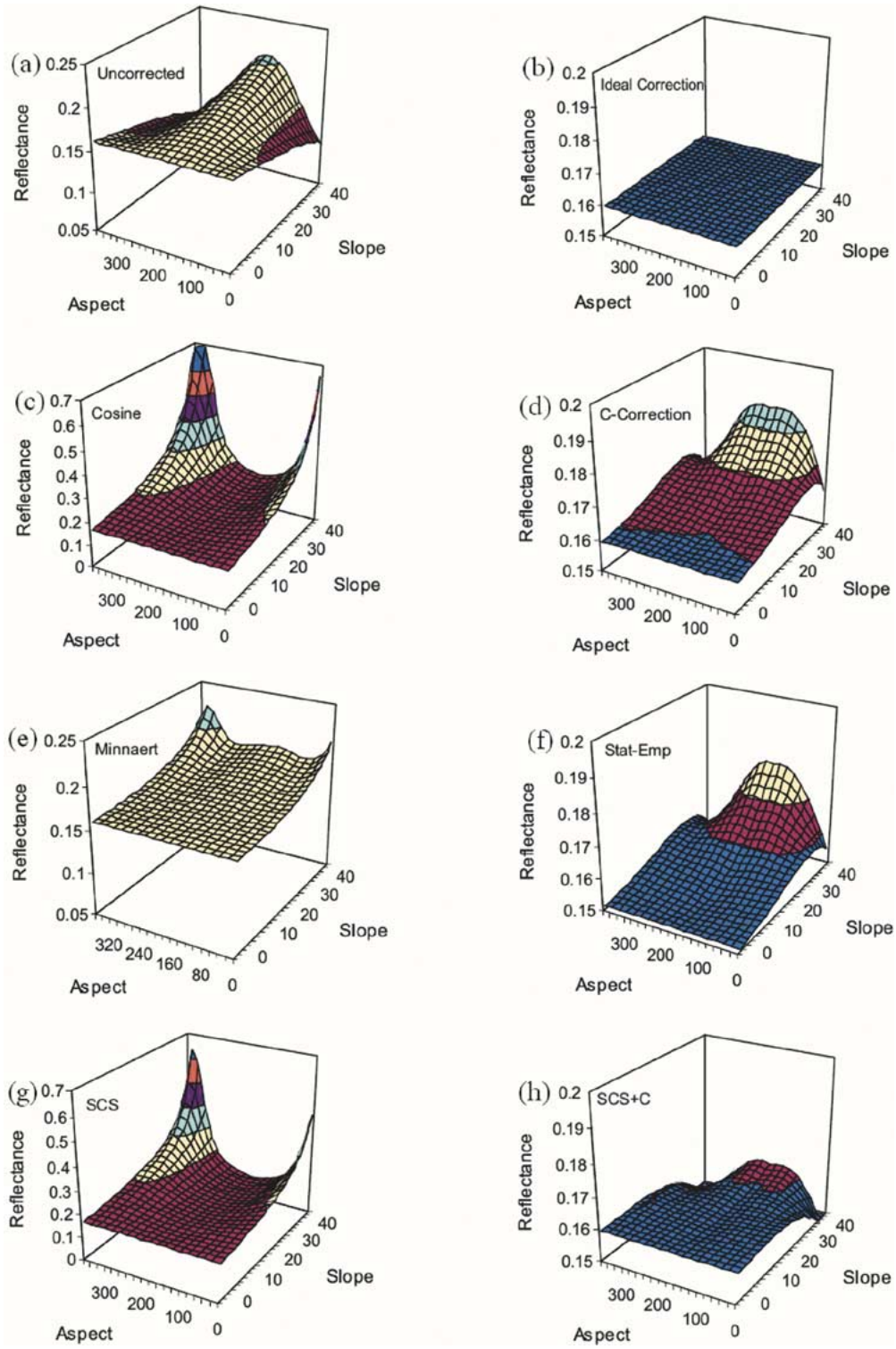


Fig. 2. Topographic corrections of modeled reflectance values over a range of terrain slopes and aspects. (a) Test dataset. GOMS-modeled reflectance values at 805 nm for lodgepole pine forest on slopes 0° to 46° (2° intervals) and full range of aspects (0° to 360° at 20° intervals) with CC held constant (70%). (b) Modeled reflectance values for ideal topographic correction. (c)–(h) Results from the following corrections: (c) cosine, (d) C-correction, (e) Minnaert, (f) statistical-empirical, (g) sun-canopy-sensor (SCS). (h) SCS+C. Principal plane is at 154°.

not account for shadow cast from neighboring terrain features (e.g., [15] and [16]).

The GOMS model provided the basis for independent and controlled testing by enabling the creation of a comprehensive set of reflectance data for a constant set of structural parameters over a full range of terrain and crown closure (CC) settings. The full set of GOMS-modeled reflectance values are shown in Fig. 2(a) for all modeled slopes and aspects (60% CC shown in this example), with the corresponding (validation) reflectance values generated for flat terrain shown in Fig. 2(b).

Validation was performed by applying each of the topographic corrections to the GOMS-modeled reflectance value

for a sloped surface, and comparing the topographically corrected reflectance value to the GOMS-modeled reflectance obtained for a flat surface, where all other canopy model inputs were held constant (i.e., identical component spectra, forest structure, and illumination conditions for both the sloped and flat cases).

This model-based context is more comprehensive for validation compared to an image-based dataset, which can only test a limited number of terrain orientations. A proper validation should consider a complete set of different slopes, aspects, and other forest stand attributes. In the past, validation has been based on one of four types of assessment: 1) visual assessment of the removal of the appearance of relief in satellite imagery [9], [12], [17], [19], [20], [30]; 2) variance statistics based on the relationship between recorded signal and the cosine of the incidence angle [1], [2], [5], [9]–[13], [30]; 3) classification results and accuracy [2], [9], [17], [19]–[21], [23], [30]; and 4) improvements in biophysical parameter prediction [8], [21], [22]. However, classification and biophysical parameter estimation assessments are only able to provide a relative assessment of the correction method and are unable to quantify the degree to which the topographic effect has been reduced. Also, variance statistics based on image datasets are limited to a subset of terrain as a function of the local environment, and even for the terrain being considered, it is difficult or impossible to know what constitutes a "correct" value on a pixel-by-pixel basis where the topographic effect is removed, and it is also difficult to locate reference validation pixels on flat terrain (elsewhere in the image) where forest structure and other stand attributes are consistent between horizontal and sloped terrain. This model-based approach to topographic correction validation presented here is therefore preferred over approaches in which the actual correct values are unknown, and in cases where the ability to assess a comprehensive range of different terrain orientations and forest structures is often limited, impractical, or both. Providing the canopy reflectance model deals with topography properly (e.g., GOMS), a more appropriate, rigorous, and consistent approach for terrain correction validation is provided.

### B. Mountain Forest Test Area

Forest physical structural parameters and endmember signature inputs for the GOMS model were obtained for a montane/subalpine forest ecoregion in Kananaskis Country along the eastern slopes of the Rocky Mountains in Alberta, Canada. As in previous studies [7], [26], [27], three endmembers were used: sunlit canopy, sunlit background, and shadow. Endmember reflectance values in the green (550 nm), red (664 nm), and near-infrared (NIR: 805 nm) were obtained for sunlit and shaded Lodgepole Pine, a dominant species in the Kananaskis region, as well as for a grass and mixed forb background. The forest structural inputs to the GOMS model are shown in Table I. The model input solar zenith angle (39.31°) and solar azimuth angle (154.32°) corresponded to midday (near solar noon) conditions near the peak of the growing season for the Kananaskis region. A series of model runs were conducted by varying slope, aspect, and crown closure to simulate a full set of results for a variety of different terrain and forest structural situations. Slope values were varied between 0° and 46° at 2° intervals, aspect was varied over the full 360° range, using a 20° increment, and crown closure was varied between 10% and 90% CC at 10% increments. The GOMS model was run multiple times in forward mode (MFM) [27], [28] to generate reflectance values for each possible combination of terrain slope, aspect, and CC for the different wavelengths. In total

$$24 \text{ different slopes} \times 19 \text{ aspects} \times 9 \text{ CC} \times 3 \text{ wavelengths} = 12\,312 \text{ different model runs}$$

were performed, with all model inputs and the corresponding forward mode reflectance value output from each model run computed and stored in a multiple forward-mode lookup table (MFM-LUT) that is suitable for follow-on statistical analysis and graphical display of results. In separate tests, slope, aspect, and CC were isolated and varied from the computed MFM-LUT, with all other parameters held constant to facilitate a series of controlled experiments.

TABLE I
GOMS MODEL INPUTS, INCLUDING MULTIPLE-FORWARD MODE (MFM-GOMS) MODEL RANGES, AND INCREMENTS FOR THE THREE PARAMETERS EVALUATED FOR A ROCKY MOUNTAIN TEST SITE, KANANASKIS ALBERTA, CANADA

| Parameter | Range | Increment |
|---|---|---|
| Slope | 0 - 46° | 2° |
| Aspect | 0 - 360° | 20° |
| Crown Closure (CC) | 10-90% | 10% |
| Horizontal Crown Radius (r) | 0.8m | - |
| Vertical Crown Radius (b) | 3.0m | - |
| Height to Crown (h) | 13.6m | - |
| Height Distribution (dh) | 8.16m | - |
| SZA | 39.31° | - |
| Solar Azimuth | 154.32° | - |

The cosine, Minnaert, statistical-empirical, C, SCS, and SCS+C corrections were applied to the full GOMS-modeled reflectance dataset and compared both graphically and statistically. In an ideal correction, the variation in the original data [Fig. 2(a)] caused by the influence of terrain would be reduced to zero since all reflectance values would be identical to those for horizontal terrain [modeled 0° slope; Fig. 2(b)] for a given set of forest stand and structural attributes. Validation was achieved by assessing the results from each correction method against this ideal (modeled) correction.

### C. Validation Tests

The experiment was organized into a series of tests that considered three fundamental dimensions of reflectance variation: topographic, spectral, and structural (Table II). Using the GOMS model, topographic variation was tested by varying slope and aspect, with spectral variations tested using different modeled wavelengths. Forest structure was tested with respect to varying crown closure, a primary structural feature of forest stands that drives reflectance change. The other structural parameters were held constant and were representative of the study site. In addition to this, a series of tests was completed using different structural inputs to the model and the results showed less variation compared with CC. Therefore, given

TABLE II
ORGANIZATION OF EXPERIMENTAL DESIGN INVOLVING THE MAIN DIMENSIONS OF REFLECTANCE VARIATION IN FOREST STANDS: TOPOGRAPHY (SLOPE, ASPECT); SPECTRAL (WAVELENGTH: $\lambda$); AND FOREST STRUCTURE (HERE, CROWN CLOSURE: CC). EACH TEST IS DESCRIBED IN THE SECTIONS OF THE PAPER INDICATED, TOGETHER WITH ITS ACCOMPANYING FIGURE, THE PRIMARY AND SECONDARY TEST VARIABLES, AND THE MODEL-BASED PARAMETERS THAT WERE HELD CONSTANT IN THESE CONTROLLED EXPERIMENTS. ADDITIONAL PARAMETERS HELD CONSTANT INCLUDE SEVERAL FOREST STRUCTURE PARAMETERS AND SOLAR POSITION (TABLE I)

| **Section in paper:** | 4.1 | 4.2 | 4.3 | 4.4 |
|---|---|---|---|---|
| **Figure:** | 2 | 3 | 4 | 5 |
| **Test approach:** | Visual: 3-D Plots | Reflectance Difference | RMSE | Reflectance Difference |
| **Primary Test Variable:** | Slope, Aspect | Slope, Aspect | $\lambda$ | CC |
| **Secondary Test Variable:** | - | CC | CC | Slope, Aspect |
| **Parameters held constant:** | CC, $\lambda$ | $\lambda$ | - | $\lambda$ |

the extensive set of tests presented, additional experiments involving altering other structural inputs (e.g., $r$, $b$, $dh$—Table I) were deemed unnecessary. We note, however, that it is possible to alter and test these or any of the other model inputs using the MFM approach [27]–[29].

In this study, we have captured the main properties of forest stands that influence reflectance using a series of comprehensive MFM-GOMS model runs, and we test these in a variety of ways to provide a rigorous validation. Four experiments were performed (Figs. 2–5; Table II), each using a different graphical and/or statistical approach, and each involving different primary and/or secondary test variables. In experiments involving both primary and secondary variables, a series of individual tests was conducted, where for each test all but one variable was held constant. However, for reporting purposes, in some cases more than one set of results were combined into a single figure to show a variety of outputs and enable more comprehensive assessments. This provided a rigorous basis to evaluate and compare the various topographic corrections, as summarized in Table II, and described in the following sections.

## IV. RESULTS

### A. Analysis of Topography

In the first validation experiment (Fig. 2), only slope and aspect were altered, with CC (70%) and wavelength (805 nm) held constant. Results are shown graphically as three-dimensional plots depicting modeled and corrected reflectance over a full range of slope and aspects. The modeled reflectance in Fig. 2(a) shows the variation of reflectance for forested terrain as a result of differing terrain slope and aspect, and represents the original

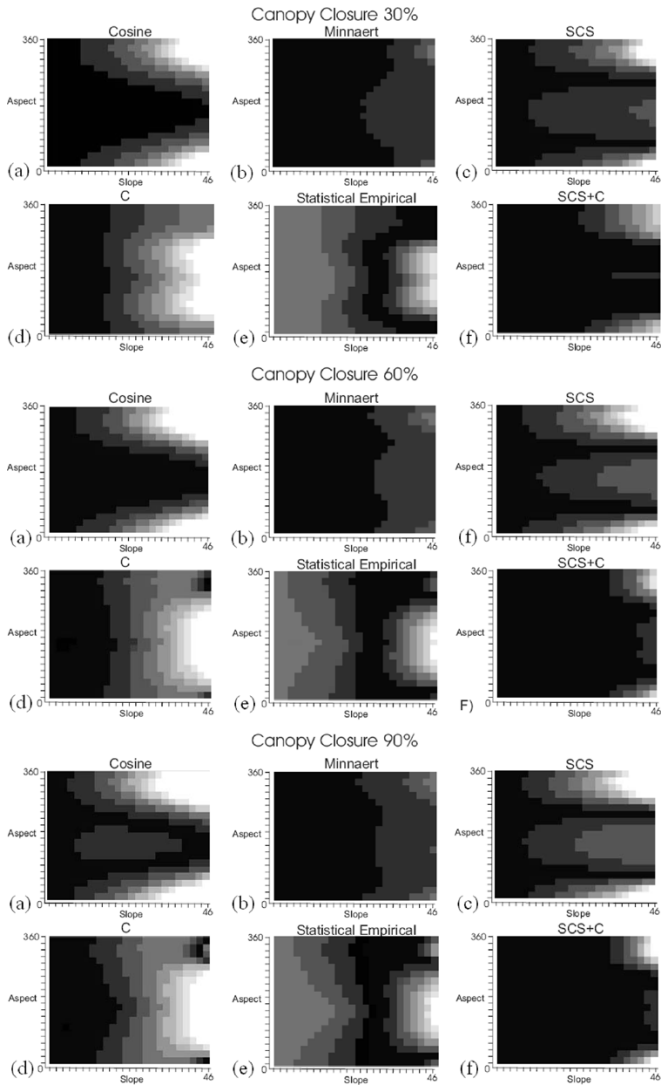


Fig. 3. Difference in reflectance between topographically corrected reflectance and known horizontal terrain reflectance value at three levels of CC and at 805 nm for the following corrections: (a) cosine, (b) Minnaert, (c) SCS, (d) C-correction, (e) statistical empirical, (f) SCS+C. Differences range from $\pm 1\%$ reflectance (darkest) to $> \pm 15\%$ reflectance (white) for A, B, and C and $\pm 0.25\%$ reflectance to $> \pm 2\%$ reflectance for D, E, and F.

"uncorrected" dataset to which the topographic corrections were applied.

The theoretical ideal correction is shown in Fig. 2(b), in which the model inputs were unchanged, except for slope which was set to zero, thus generating topographically normalized reflectance values that were used for independent validation. Validation was achieved by comparing the model-based topographically normalized reflectance values with the reflectance values output from the six topographic corrections studied [cosine, Minnaert, C, statistical-empirical, SCS, SCS+C; see Fig. 2(c)–(h)]. These graphics facilitate comprehensive visual assessment of the full range of topography, and the various corrections applied. In Fig. 2, only NIR reflectance results are shown; however, results at other wavelengths appeared similar (corrections at different wavelengths are evaluated in Section IV-C). In all cases, the variation in reflectance was most pronounced near the principal plane of illumination

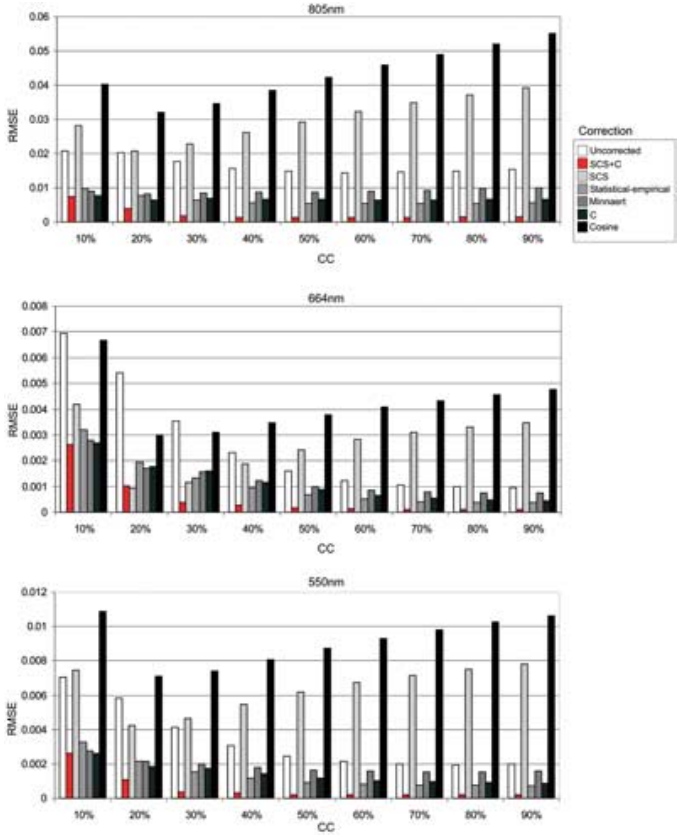


Fig. 4. RMSE between the modeled reflectance values for horizontal terrain (validation) and various topographically corrected reflectances at three positions in the electromagnetic spectrum: (top) NIR: 805 nm, (middle) red: 664 nm, (bottom) green: 550 nm and for CCs ranging from 20% to 100%. Results from SCS+C shown in red for ease of comparison with other methods.

(terrain aspect $=$ 160°, 340°), and especially at steep slope angles.

With the uncorrected reflectance data [Fig. 2(a)], higher reflectance values corresponded with terrain orientations facing the source of illumination. In these terrain settings, a greater proportion of canopy is exposed to direct illumination compared to the same forest setting on flat terrain, and furthermore, cast shadow is projected upslope, thus shortening or in some cases completely obscuring the shadow component.

The increased sunlit canopy fraction and the reduced shadow fraction both contribute to higher reflectance values compared to the reflectance that would be obtained for an identical forest situated on a flat surface. Similarly, the lower reflectance values found for terrain facing away from the source of illumination result from the pixel becoming more dominated by shadow. In these instances, the shadow cast by upslope trees is elongated, with a greater proportion of the canopy hidden from the source of illumination. The increased shadow fraction and decreased sunlit canopy fraction result in a lower integrated pixel level reflectance.

The cosine correction [Fig. 2(c)] showed an overcorrection (maximum reflectance $= 66\%$) at slopes facing away from the source of illumination (between 230° and 80°) as a result of the unmoderated correction factor. The results of the cosine correction also showed occurrences of undercorrection (maximum reduction of 4% reflectance) for steep, sun-facing slopes.

The Minnaert correction [Fig. 2(e)] provided an improvement in the corrected values for shaded slopes. The reduction in overcorrection compared with the cosine correction is apparent for slopes opposite the direction of illumination (maximum reduction: 45% reflectance). However, the moderating effect on the correction factor also resulted in a greater undercorrection (3% reflectance) for steep, sun-facing terrain (e.g., slopes $>$ 20°, aspects 140° to 180°).

The statistical-empirical correction [Fig. 2(f)] showed an even greater reduction ($-50\%$ reflectance) in the overcorrection compared to the cosine correction; however, it too incurred undercorrection (e.g., 2% reflectance at 160° aspect, 46° slope).

The C-correction [Fig. 2(d)] showed improvements on the cosine correction similar to those of the Minnaert and statistical-empirical corrections. Of the three semiempirical corrections (C-correction, Minnaert, and statistical-empirical), the C-correction along with the statistical-empirical correction showed the smallest increase ($+2\%$ reflectance) at the maximum point of undercorrection (160° aspect, 46° slope) when compared to the cosine correction. Values for C are shown in Table III.

The SCS correction [Fig. 2(g)] was an effective correction for sun-facing terrain. However, compared to the cosine correction, which was the most effective of the sun-terrain-sensor-based corrections for sun-facing terrain, the SCS correction overcorrected at 160° aspect and 46° slope by 4% reflectance. The SCS correction also showed overcorrection features (maximum of 30% reflectance) for shaded slopes, similar to that produced by the cosine correction (e.g., 320° aspect, 46° slope). However, compared to the cosine correction, these overcorrection features began at higher slopes than the cosine correction, and were less pronounced.

The SCS+C correction [Fig. 2(h)] reduced the overcorrection compared to SCS by 32% reflectance for shaded slopes (e.g., between 230° and 80° aspects), and eliminated the overcorrection for sun facing slopes (160° aspect and 46° slope). The SCS+C correction showed a slight undercorrection for shaded slopes (1% reflectance). While the correction appeared similar to the other semiempirical methods for shaded slopes, it was improved for sun-facing terrain, an area where other corrections (e.g., statistical-empirical, C-correction) were less effective.

### *B. Reflectance Difference by Terrain and Crown Closure*

In the second validation experiment (Fig. 3; Table IV), a detailed assessment of the differences between each correction and the modeled validation reflectance data was performed for a full range of terrain slope and aspect, and at crown closures of 30%, 60%, and 90%. Wavelength was held constant at 805 nm.

Overestimation of reflectance with respect to the modeled validation surface was evident for the cosine and SCS corrections [Fig. 3(a) and (c)] at high CCs with maximum differences of 55% reflectance and 45% reflectance, respectively. The SCS correction also showed a considerable amount of negative difference (5% reflectance). The SCS and cosine corrections resulted in the lowest number of slope-aspect combinations with reflectance within 1% of the modeled validation data (Table IV).

The Minnaert, C, statistical-empirical and SCS+C corrections [Fig. 3(b), (d)–(f)] all showed a reduction in positive difference

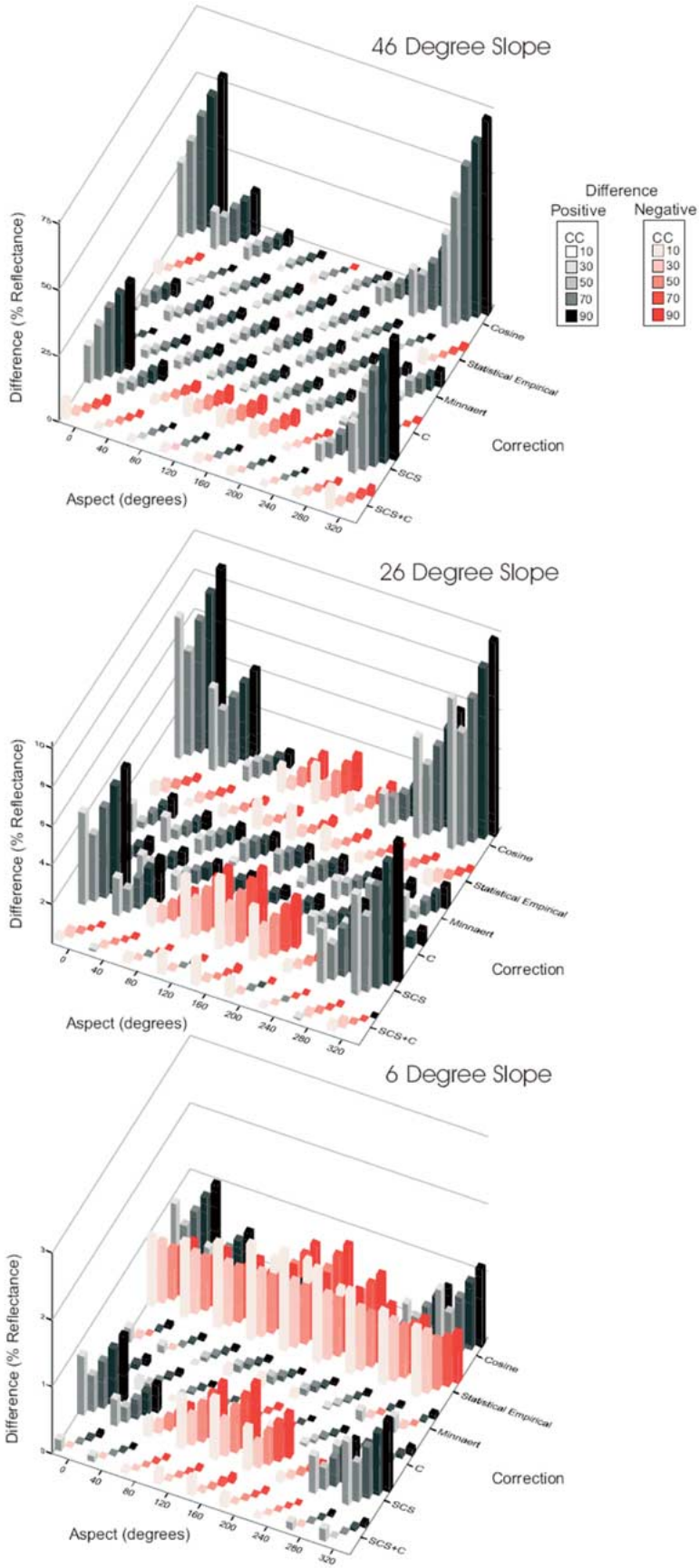


Fig. 5. Difference in NIR (805 nm) reflectance between the modeled reflectance values for horizontal terrain (validation) and various topographically corrected reflectances for CCs of 10%, 30%, 50%, 70%, and 90% at 40° aspect intervals for slopes of (bottom) 6°, (middle) 26°, and (top) 46°. Red scale bars indicate a negative difference, and grayscale bars indicate a positive difference [correction–validation].

TABLE III
C VALUES BY BAND AND CROWN CLOSURE

| | Wavelength | | |
|---|---|---|---|
| CC | *Green* | *Red* | *NIR* |
| 10 | 0.50 | 0.30 | 0.63 |
| 20 | 0.37 | 0.09 | 0.51 |
| 30 | 0.57 | 0.17 | 0.64 |
| 40 | 0.90 | 0.42 | 0.82 |
| 50 | 1.26 | 0.77 | 0.98 |
| 60 | 1.55 | 1.15 | 1.09 |
| 70 | 1.74 | 1.46 | 1.16 |
| 80 | 1.85 | 1.64 | 1.21 |
| 90 | 1.88 | 1.76 | 1.24 |

TABLE IV
PERCENTAGE OF SLOPE ASPECT COMBINATIONS WITH CORRECTED DATA WITHIN 1% REFLECTANCE OF MODELED VALIDATION DATA. RESULTS ARE PRESENTED FOR ALL SLOPE ASPECT COMBINATIONS AND SLOPE ASPECT COMBINATIONS WHERE SLOPE EXCEEDS 20°. BEST RESULT FOR EACH CASE SHOWN IN BOLD

| | Percentage within 1% Difference of Validation | | | Percentage within 1% Difference for steep terrain (slope >20°). | | |
|---|---|---|---|---|---|---|
| | *30% CC* | *60% CC* | *90% CC* | *30% CC* | *60% CC* | *90% CC* |
| Cosine | 51 | 45 | 38 | 32 | 28 | 2 |
| Minnaert | 67 | 64 | 62 | 39 | 34 | 29 |
| C-correction | 75 | 77 | 76 | 54 | 58 | 56 |
| Statistical Empirical | 92 | 93 | 92 | 86 | 87 | 85 |
| SCS | 44 | 36 | 31 | 18 | 13 | 11 |
| SCS+C | **95** | **98** | **97** | **91** | **96** | **94** |

when compared to the cosine and SCS corrections, with the SCS+C and statistical-empirical corrections showing the lowest levels of overall difference. The SCS+C and statistical-empirical corrections were more effective for a higher number of slope aspect combinations (Table IV). In particular, the SCS+C correction appeared to be most effective across all CC levels [Fig. 3(f); Table IV], and never exceeded 3% difference, the lowest maximum difference for all corrections tested.

### C. Analysis of Different Wavelengths and Crown Closures

The third validation experiment (Fig. 4) focused primarily on assessing different wavelengths, with a secondary analysis of a detailed set of CCs (Table II). The analysis used a root mean square error (RMSE) value computed for each correction to determine the overall residual between the various corrected data values and the modeled (validation) horizontal terrain values at green (550 nm), red (664 nm), and NIR (805 nm) wavelengths. The RMSE for the uncorrected NIR data was between 0.015 and 0.02 over the range of CC (10% to 90%). The cosine correction consistently had the highest level of RMSE throughout the range of CCs and for all wavelengths tested. Over the set of CCs, the RMSE for the cosine correction ranged from 0.032 to 0.055 (NIR), 0.0030 to 0.0066 (red), and 0.0071 to 0.0109 (green). This error was consistently greater than that of the uncorrected data, indicating that the level of variation in the data compared with horizontal terrain reflectance was higher in the cosine corrected data than the uncorrected data. This is related to the severe overcorrections that resulted due to its inability to characterize diffuse radiation properly. This was also observed for the SCS correction, especially at green and red wavelengths and at higher CCs (Fig. 4).

The Minnaert correction and C-correction had similar RMSEs for CCs greater than 40% at all three wavelengths. The statistical-empirical correction data had a lower RMSE than the other semiempirical corrections, with RMSEs over the full set of CCs ranging from 0.0053 to 0.0096 (NIR), 0.0004 to 0.0031 (red), and 0.0007 to 0.0033 (green).

The SCS+C corrected data had the lowest RMSE for all CCs at all wavelengths, with the exception of 20% CC at 664 nm. The SCS+C RMSE ranges at all CCs were 0.0012 to 0.0075 (NIR), 0.0001 to 0.0026 (red), and 0.0002 to 0.0026 (green).

### D. Analysis of Crown Closure Over Different Terrain

The fourth validation test (Fig. 5) was a detailed examination of crown closure over a full range of terrain aspects at low (6°), moderate (26°) and high (46°) slopes at the NIR (805 nm) wavelength. The effect of CC on correction efficacy varied with the correction method used. The cosine correction showed higher levels of difference with increasing CC, especially at higher slopes. The exception to this was aspects facing away from the source of illumination, where the cosine corrected data had larger differences at lower CCs (e.g., 10% CC). The Minnaert corrections had the lowest differences at CCs of 10% while the level of difference was similar among CC levels higher than 30%. The C-correction and SCS+C corrections were similar to the Minnaert correction in that the 10% CC corrected data showed less difference than at higher levels of CC. At a slope of 6°, the statistical-empirical corrected data had the most variation over the different aspects (maximum difference of $-1.5\%$ reflectance).

At steeper slopes, as CC increased, the corrected data had more variation with aspect, with the smallest differences in the principal plane of illumination (160° aspect). Also, at these moderate slopes (26°), the statistical-empirical correction was similar to the other semiempirical corrections, while at higher CCs, the magnitude of difference was lower (maximum of 0.33% reflectance at 90% CC). The SCS corrected data were similar to the cosine corrected data in that they displayed a level of difference for 10% CC at moderate and high slopes that was greater than at higher CCs at aspects facing the source of illumination.

The SCS+C method produced the lowest average differences across all aspects for all CCs. The SCS+C corrections had trends similar to the other semiempirical corrections, with the SCS+C corrections at higher CCs showing lower magnitudes of difference compared to the other corrections. At lower slopes, there were more occurrences of undercorrection (shown in red in Fig. 5) compared to moderate and high slopes for all corrections tested.

## V. DISCUSSION

The results from the terrain correction experiments demonstrated that some of the radiometric variation caused by terrain slope and aspect can be reduced using simple photometric equations and semiempirical constants, but that the physically based approaches that account for vegetation structure (e.g., SCS, SCS+C) are more appropriate for forested terrain. The SCS and SCS+C corrections are theoretically more sound owing to their proper representation of geotropic tree structure. They are also superior as they account for subpixel scale sunlit canopy

components with respect to the angles of solar illumination, sensor view, and terrain slope. These methods provided improved corrections over a more full range of terrain orientations. Each of the earlier correction techniques (Minnaert, C, cosine, statistical-empirical) appear to have slope-aspect combinations where they are effective, but fail beyond these. In general, corrections based on canopy physical structure (SCS) and that include a semiempirical constant to compensate for low levels of direct illumination (SCS+C) were more effective at reducing the level of data variation across all slope-aspect combinations.

All correction methods appeared to be less effective for steeper terrain (slopes $> 20°$) with the exception of the statistical-empirical correction. In particular, the cosine correction and SCS correction were unsuitable for steep slopes facing away from the source of illumination. The level of difference between the corrected reflectance values and the validation reflectance modeled for flat terrain for these situations was very large (Fig. 3) for all CCs. For both corrections (cosine, SCS), the terrain-induced variation in the corrected data was higher than for the original uncorrected data. This occurred for shadow-dominated pixels where the angle of incidence ($i$) approached 90°. In these cases, the denominator in the correction factor $\cos(i)$ approached zero, thus creating large overcorrections due to the high correction factors (e.g., SCS correction factor: 5.6 at 46° slope, 320° aspect). The introduction of the C parameter in SCS+C reduced this overcorrection considerably (e.g., SCS+C correction factor $= 2.6$ at 46° slope, 320° aspect).

In steep terrain, the corrections that most effectively reduced the terrain-induced reflectance variations were those that either made use of a moderating factor (Minnaert, C, SCS+C) or used a statistical approach. These corrections were more effective at certain slope-aspect combinations than at others. For example, the SCS+C method was more effective than the statistical-empirical method for correcting steep slopes facing the direction of illumination (Figs. 2 and 3), whereas the statistical-empirical method was more effective at correcting slopes facing away from the direction of illumination. However, at low and moderate slopes (e.g., $< 26°$), the SCS+C correction showed lower levels of difference for both situations.

The SCS+C correction was the most effective overall in terms of suitability over the full range of terrain and crown closures considered in this study (Figs. 2–5). Set in the improved, physically based sun-canopy-sensor (SCS) framework [5], the SCS+C correction we have introduced preserves the capabilities of SCS and provides improved results in terrain situations where SCS was less effective.

The SCS correction was shown to be effective across a variety of terrain orientations, and even at high slopes in the principle plane; however it has a distinct overcorrection problem on higher slopes facing away from the illumination source. This problem is addressed in SCS+C using a semiempirical moderator representing diffuse irradiance on shaded slopes, making it effective for the entire range of slope-aspect combinations. The effectiveness of SCS+C is also not compromised in situations where SCS already works well. In those cases, the addition of the C factor makes little or no difference and the SCS+C correction essentially reverts to the fundamental SCS formulation. Other correction methods were slightly more effective for a small number of specific slope-aspect combinations, but none were markedly more effective than the SCS+C (Figs. 3 and 5).

Existing photometric methods provide a simple and effective way to reduce the variation in data caused by the topographic effect. However, these existing correction methods are generally not stable over a wide range of slope-aspect combinations or angles of incidence. Ideally, in forested terrain, a normalization method would provide an appropriate framework that accurately represents the physical structure of tree growth, and permits normalization of the subpixel scene fractions [8]—and it would be stable over the full range of terrain slopes and aspects as well as forest structural conditions. The SCS correction provides an appropriate framework for this, with the SCS+C modification providing a more robust implementation that enables this concept to be available over a much broader range of terrain and structural settings.

In addition to introducing SCS+C as a new and more effective topographic correction approach in forested terrain, this paper also makes a more general contribution of an improved method for experimental testing and validation of topographic corrections based on use of independent geometric optical canopy reflectance models. In previous papers [1], [2], [5], [9]–[13], [30], this has been an issue owing to a variety of *ad hoc* methods that generally involved limited comparisons and little basis for comprehensive validation of topographic correction results. In these studies, it was often difficult, impractical or impossible to know what the correct topographically normalized value should be for a particular slope-aspect geometry or forest structure.

Use of powerful canopy geometric optical reflectance models provides a framework for topographic correction validation that is: 1) independent of any of the correction methods; 2) comprehensive in that a full range of terrain and forest conditions can be tested using multiple-forward mode (MFM) model runs [27], [28]; and 3) for a given slope-aspect terrain setting, the topographically corrected reflectance value can be obtained by simply altering the terrain settings to the flat surface and rerunning the model. This latter point has led to the development of topographic corrections for spectral mixture analysis scene fractions [8] and an explicit model-based topographic correction method [29]. Models such as the Li–Strahler geometric optical mutual shadowing [14] model are recommended for these purposes, since they explicitly account for terrain, have a physical-structural basis and have been shown [7] to provide improved results compared to other models while maintaining a manageable set of input parameters suitable for larger area studies, and they are also amenable to newer model-based inversion schemes such as MFM [27], [28].

## VI. Conclusion

In forested terrain, topography modifies the sun-sensor-surface geometry, causes changes in the subpixel scale scene fractions, and causes variation in the signal recorded at the sensor. This topographic effect was modeled using the GOMS canopy reflectance model in multiple-forward mode by varying terrain

and crown closure inputs. This modeled-based approach provided a more appropriate, rigorous, and comprehensive framework for the comparison, testing, and validation of different topographic correction methods compared to previous validation methods and is therefore recommended for topographic correction validation in forested terrain.

Physically based corrections that preserve the sun-canopy-sensor geometry (SCS, SCS+C) while adjusting for terrain represent a more realistic and effective approach to topographic correction. Earlier methods ignore the geotropic nature of tree growth and the effect that the complex interaction between terrain and scene component fractions has on reflectance at subpixel scales. However, the original SCS approach, while accounting for these critical growth and terrain interactions, overcorrects reflectance as the angle of incidence approaches 90°. The result is uncharacteristically large reflectance values for slopes facing away from the source of illumination, thus limiting the overall utility of the SCS approach. In the SCS+C method introduced here, the addition of the semiempirical moderator (C) to the SCS correction reduced this overcorrection, building on earlier improvements provided by the C-correction to the original cosine correction formulation. In a series of controlled experiments involving comprehensive assessments of slope, aspect, and crown closure, the SCS+C correction was shown to provide improved corrections over a greater range of terrain and forest structural conditions compared to SCS, particularly in steeper terrain and for slopes facing away from the sun. SCS+C was also shown to be superior to existing and widely accepted correction techniques (cosine, C, Minnaert, statistical-empirical). The addition of the C parameter to the SCS formulation is simple to derive and based on well-known and established topographic correction concepts [1]–[3] that we have now applied to an improved correction framework [5]. Accordingly, it is recommended that SCS+C be considered for topographic correction of remote sensing imagery of forested terrain.

## ACKNOWLEDGMENT

Computing resources were provided through the Westgrid/Netera/Multimedia Advanced Computational Infrastructure available through the University of Lethbridge.

## REFERENCES

[1] C. O. Justice, S. W. Wharton, and B. N. Holben, "Application of digital terrain data to quantify and reduce the topographic effect on Landsat data," *Int. J. Remote Sens.*, vol. 2, no. 3, pp. 213–230, 1981.

[2] P. M. Teillet, B. Guindon, and D. G. Goodenough, "On the slope-aspect correction of multispectral scanner data," *Can. J. Remote Sens.*, vol. 8, no. 2, pp. 84–106, 1982.

[3] J. A. Smith, T. L. Lin, and K. J. Ranson, "The Lambertian assumption and Landsat data," *Photogramm. Eng. Remote Sens.*, vol. 46, no. 9, pp. 1183–1189, 1980.

[4] H. Hugli and W. Frei, "Understanding anisotropic reflectance in mountainous terrain," *Photogramm. Eng. Remote Sens.*, vol. 49, no. 5, pp. 671–683, 1983.

[5] D. Gu and A. Gillespie, "Topographic normalization of Landsat TM images of forest based on subpixel sun-canopy-sensor geometry," *Remote Sens. Environ.*, vol. 64, pp. 166–175, 1998.

[6] F. G. Hall, Y. E. Shimabukuro, and K. F. Huemmerich, "Remote sensing of forest biophysical structure using mixture decomposition and geometric reflectance models," *Ecol. Appl.*, vol. 5, no. 4, pp. 993–1013, 1995.

[7] D. R. Peddle, F. G. Hall, and E. F. LeDrew, "Spectral mixture analysis and geometric-optical reflectance modeling of boreal forest biophysical structure," *Remote Sens. Environ.*, vol. 67, pp. 288–297, 1999.

[8] R. L. Johnson, D. R. Peddle, and R. J. Hall, "A modeled-based sub-pixel scale mountain terrain normalization algorithm for improved LAI estimation from airborne CASI imagery," in *Proc. 22nd Can. Symp. Remote Sensing*, Victoria, BC., Canada, Aug. 21–25, 2000, pp. 415–424.

[9] P. Meyer, K. I. Itten, T. Kellenberger, S. Sandmeier, and R. Sandmeier, "Radiometric corrections of topographically induced effects on Landsat TM data in an alpine environment," *ISPRS J. Photogramm. Remote Sens.*, vol. 48, no. 4, pp. 17–28, 1993.

[10] F. Cavayas, "Modeling and correction of topographic effect using multitemporal satellite images," *Can. J. Remote Sens.*, vol. 13, no. 2, pp. 49–67, 1987.

[11] J. D. Colby, "Topographic normalization in rugged terrain," *Photogramm. Eng. Remote Sens.*, vol. 57, no. 5, pp. 531–537, 1991.

[12] D. L. Civco, "Topographic normalization of Landsat Thematic Mapper digital imagery," *Photogramm. Eng. Remote Sens.*, vol. 55, no. 9, pp. 1303–1309, 1989.

[13] M. Vincini and E. Frazzi, "Multitemporal evaluation of topographic normalization methods on deciduous forest TM data," *IEEE Trans. Geosci. Remote Sens.*, vol. 41, no. 11, pp. 2586–2590, Nov. 2003.

[14] X. Li and A. H. Strahler, "Geometric-optical bidirectional reflectance modeling of the discrete crown vegetation canopy: Effect of crown shape and mutual shadowing," *IEEE Trans. Geosci. Remote Sens.*, vol. 30, no. 2, pp. 276–292, Mar. 1992.

[15] C. Proy, D. Tanré, and P. Y. Deschamps, "Evaluation of topographic effects in remotely sensed data," *Remote Sens. Environ.*, vol. 30, pp. 21–32, 1989.

[16] D. S. Kimes and J. A. Kirchner, "Modeling the effects of various radiant transfers in mountainous terrain on sensor response," *IEEE Trans. Geosci. Remote Sens.*, vol. GE-19, pp. 100–108, Jan. 1981.

[17] C. Conese, M. A. Gilabert, F. Maselli, and L. Bottai, "Topographic normalization of TM scenes through the use of an atmospheric correction method and digital terrain models," *Photogramm. Eng. Remote Sens.*, vol. 59, no. 12, pp. 1745–1753, 1993.

[18] M. Minnaert, "The reciprocity principle in lunar photometry," *Astrophys. J.* , vol. 93, pp. 403–410, 1941.

[19] K. I. Itten and P. Meyer, "Geometric and radiometric correction of TM data of mountainous forested areas," *IEEE Trans. Geosci. Remote Sens.*, vol. 31, no. 4, pp. 764–770, Jul. 1992.

[20] J. D. Colby and P. L. Keating, "Land cover classification using Landsat TM imagery in the tropical highlands: The influence of anisotropic reflectance," *Int. J. Remote Sens.*, vol. 19, no. 8, pp. 1479–1500, 1998.

[21] T. Tokola, J. Sarkeala, and M. V. D. Linden, "Use of topographic correction in Landsat TM-based forest interpretation in Nepal," *Int. J. Remote Sens.*, vol. 22, no. 4, pp. 551–563, 2001.

[22] S. Ekstrand, "Landsat TM-based forest damage assesment: Correction for topographic effects," *Photogramm. Eng. Remote Sens.*, vol. 62, no. 2, pp. 151–161, 1996.

[23] D. Riano, E. Chuvieco, J. Salas, and I. Aguado, "Assessment of different topographic corrections in Landsat-TM data for mapping vegetation types," *IEEE Trans. Geosci. Remote Sens.*, vol. 41, no. 5, pp. 1056–1061, May 2003.

[24] D. Gu and A. Gillespie, "Response to Dymond and Shepard's comment on 'Topographic normalization of Landsat TM images of forest based on subpixel sun-canopy-sensor geometry'," *Remote Sens. Environ.*, vol. 69, pp. 195–196, 1999.

[25] C. B. Schaff, X. Li, and A. H. Strahler, "Topographic effects on bidirectional and hemispherical reflectances calculated with a geometric-optical canopy model," *IEEE Trans. Geosci. Remote Sens.*, vol. 32, no. 6, pp. 1186–1192, Nov. 1994.

[26] D. R. Peddle and R. L. Johnson, "Spectral mixture analysis of airborne remote sensing imagery for improved prediction of leaf area index in mountainous terrain, Kananaskis Alberta," *Can. J. Remote Sens.*, vol. 26, no. 3, pp. 176–187, 2000.

[27] D. R. Peddle, S. E. Franklin, R. L. Johnson, M. A. Lavigne, and M. A. Wulder, "Structural change detection in a disturbed conifer forest using a geometric optical reflectance model in multiple-forward mode," *IEEE Trans. Geosci. Remote Sens.*, vol. 41, no. 1, pp. 163–166, Jan. 2003.

[28] D. R. Peddle, R. L. Johnson, J. Cihlar, and R. Latifovic, "Large area forest classification and biophysical parameter estimation using the 5-scale canopy reflectance model in multiple-forward mode," *Remote Sens. Environ.*, vol. 89, no. 2, pp. 252–263, 2004.

[29] S. A. Soenen, D. R. Peddle, and C. Coburn, "Topographic correction of remote sensing imagery using a canopy reflectance model," presented at the *25th Can. Symp. Remote Sensing*, Montreal, QC, Canada, Oct. 14–17, 2003, p. 10.

[30] D. Gu, A. R. Gillespie, J. B. Adams, and R. Weeks, "A statistical approach for topographic correction of satellite images by using spatial context information," *IEEE Trans. Geosci. Remote Sens.*, vol. 37, no. 1, pp. 236–246, Jan. 1998.

[31] J. R. Dymond and J. D. Shepard, "Comment on 'Topographic normalization of Landsat TM images of forest based on subpixel sun-canopy-sensor geometry' by Gu and Gillespie," *Remote Sens. Environ.*, vol. 64, pp. 166–175, 1999.

[32] F. Gemmell, "An investigation of terrain effects on the inversion of a forest reflectance model," *Remote Sens. Environ.*, vol. 65, pp. 155–169, 1998.

[33] P. Scarth and S. Phinn, "Determining forest structural attributes using an inverted geometric-optical model in mixed Eucalypt forests, Southeast Queensland, Australia," *Remote Sens. Environ.*, vol. 71, pp. 141–157, 2000.

[34] F. M. Gemmell, "Effects of forest cover, terrain, and scale on timber volume estimation with Thematic Mapper data in a rocky mountain site," *Remote Sens. Environ.*, vol. 51, no. 2, pp. 291–305, 1995.

[35] J. Franklin, F. W. Davis, and P. Lefebvre, "Thematic Mapper analysis of tree cover in semiarid woodlands using a model of canopy shadowing," *Remote Sens. Environ.*, vol. 36, pp. 189–202, 1991.

[36] J. M. Chen, X. Li, T. Nilson, and A. Strahler, "Recent advances in geometrical optical modeling and its applications," *Remote Sens. Rev.*, vol. 18, pp. 227–262, 2000.

[37] D. R. Peddle, S. P. Reid-Brunke, and F. G. Hall, "A comparison of spectral mixture analysis and ten vegetation indices for estimating boreal forest biophysical information from airborne data," *Can. J. Remote Sens.*, vol. 27, no. 6, pp. 627–635, 2001.

**Scott A. Soenen** received the B.Sc. (honors) degree in geography with a concentration in the geographical information sciences from the University of Lethbridge, Lethbridge, AB, Canada, in 2003. He is currently pursuing the M.Sc. degree at the University of Lethbridge.

He is also a Research Associate with the Prairie Adaptation Research Collaborative and Water Institute for Semi-arid Ecosystems (PARC-WISE) and the Alberta Ingenuity Centre. His research interests are in canopy reflectance modeling and remote sensing with applications in forestry and climate change.

**Derek R. Peddle** (M'02) received the B.Sc. (honors) degree in computer science and geography from Memorial University of Newfoundland, St. John's, NF, Canada, the M.Sc. degree in geography from the University of Calgary, Calgary, AB, Canada, and the Ph.D. degree in geography/remote sensing from the University of Waterloo, Waterloo, ON, Canada, in 1987, 1991, and 1997, respectively.

He holds the PARC-WISE Research Professorship in Climate Change at The University of Lethbridge, Lethbridge, AB, Canada, where he is also an Associate Professor of geography, Scientific Director of the Water Institute for Semi-arid Ecosystems (WISE), Alberta Ingenuity Centre Theme Leader, and Fluxnet-Canada Co-Investigator. Prior to joining the University of Lethbridge in 1996, he also worked at NORDCO Ltd., the Institute for Space and Terrestrial Science (now ETech/CRESTech), Wilfrid Laurier University, and the National Aeronautics and Space Administration (NASA). His NSERC-funded research program involves the development of remote sensing and GIS algorithms for studies of global environmental change, terrestrial ecosystem dynamics, and terrain modeling, with applications in forestry, agriculture, water, mountains, and ocean environments. He has participated in numerous international research programs and field campaigns and has published over 100 papers including over 40 in refereed scientific journals and six that received best paper awards at national/international symposia. He is presently on the editorial board of the *Canadian Journal of Remote Sensing*.

Dr. Peddle received a NASA Visiting Scientist Award in 1994 at the NASA Goddard Space Flight Center (GSFC) with the Universities Space Research Association. In 1999–2000, he was awarded an International Fulbright Senior Fellowship on sabbatical at the University of Maryland and the NASA GSFC Terrestrial Physics Laboratory in the Biospheric Sciences Branch, where he is presently a member of the MODIS Science Team. He was awarded the 2005–2006 Canada–U.S. Fulbright Visiting Research Chair in Fundamental and Applied Ecology at the National Center for Ecological Analysis and Synthesis at the University of California, Santa Barbara. He serves as National Vice-Chair of the Canadian Remote Sensing Society (CRSS). He is a member of CRSS, IEEE GRSS, the Canadian Association of Geographers, and the Alberta Geomatics Group. He is also the faculty representative on the University of Lethbridge Board of Governors and Senate.

**Craig A. Coburn** (M'05) received the B.Sc. degree from the University of Saskatchewan, Saskatoon, SK, Canada, the M.Sc. degree in geography from the University of Alberta, Edmonton, AB, Canada, and the Ph.D. degree in geography/remote sensing from Simon Fraser University, Burnaby, BC, Canada, in 1994, 1996, and 2002, respectively.

He was appointed Assistant Professor of geography at the University of Lethbridge, Lethbridge, AB, Canada in 2002. His primary research interests are in characterizing image texture, multiresolution data analysis, spatial statistics, and remote sensing system development with applications in forestry and terrain modeling.